

Efficient Simulation of Structural Faults for the Reliability Evaluation at System-Level

Original

Efficient Simulation of Structural Faults for the Reliability Evaluation at System-Level / Kochte, M. A.; Zoellin, C. G.; Baranowski, R.; Imhof, M. E.; Wunderlich, H. J.; Hatami, N.; DI CARLO, Stefano; Prinetto, Paolo Ernesto. - STAMPA. - (2010), pp. 3-8. (Intervento presentato al convegno IEEE 19th Asian Test Symposium (ATS) tenutosi a Shanghai, CN nel 1-4 Dec. 2010) [10.1109/ATS.2010.10].

Availability:

This version is available at: 11583/2380373 since: 2016-09-16T17:36:54Z

Publisher:

IEEE Computer Society

Published

DOI:10.1109/ATS.2010.10

Terms of use:

This article is made available under terms and conditions as specified in the corresponding bibliographic description in the repository

Publisher copyright

(Article begins on next page)

A study of the dynamics of magnetic disaccommodation in amorphous ferromagnets.

II. Theoretical considerations

P. Allia, C. Beatrice, and F. Vinai

Citation: [Journal of Applied Physics](#) **68**, 4724 (1990); doi: 10.1063/1.346153

View online: <http://dx.doi.org/10.1063/1.346153>

View Table of Contents: <http://scitation.aip.org/content/aip/journal/jap/68/9?ver=pdfcov>

Published by the [AIP Publishing](#)

Articles you may be interested in

[Ferromagnetic resonance and magnetic disaccommodation of Ti-doped single crystal lithium ferrites](#)

Appl. Phys. Lett. **67**, 427 (1995); 10.1063/1.114621

[A study of the dynamics of magnetic disaccommodation in amorphous ferromagnets. I. Experimental results](#)

J. Appl. Phys. **68**, 4719 (1990); 10.1063/1.346152

[Evidence for correlations among the ordering processes responsible for the permeability disaccommodation in amorphous ferromagnets](#)

J. Appl. Phys. **63**, 829 (1988); 10.1063/1.340076

[Dynamic observation of magnetic domains in amorphous ferromagnetic ribbons driven at line frequencies](#)

Appl. Phys. Lett. **51**, 376 (1987); 10.1063/1.98447

[Magnetic Transition of Wurster's Blue Perchlorate. II. Theoretical Considerations](#)

J. Chem. Phys. **47**, 401 (1967); 10.1063/1.1711908

The logo for the AIP Journal of Applied Physics. It features the letters 'AIP' in a large, white, sans-serif font on the left. To its right is a vertical orange bar, followed by the words 'Journal of Applied Physics' in a smaller, white, sans-serif font. The background is a dark orange with a subtle, swirling pattern.

Meet The New Deputy Editors



Christian
Brosseau



Laurie
McNeil



Simon
Phillpot

A study of the dynamics of magnetic disaccommodation in amorphous ferromagnets. II. Theoretical considerations

P. Allia

Physics Department, Politecnico di Torino, Torino, Italy and GNSM-CISM, Torino, Italy

C. Beatrice and F. Vinai

Istituto Elettrotecnico Nazionale "Galileo Ferraris," and GNSM-CISM, Torino, Italy

(Received 17 July 1989; accepted for publication 21 June 1990)

The results obtained in part I are interpreted in terms of the viscosity field arising from independent processes of directional ordering for magnetic defects dispersed in the amorphous structure and interacting with the magnetization vector. A specific model is developed in order to take into account the changes in the ordering kinetics induced by the periodic magnetization rotations described in part I. This model, however, requires that the magnetic induction remain constant during the whole measurement; as a consequence, the model's predictions cannot be directly compared with the experimental results, obtained instead at constant applied field. This difficulty is overcome by deriving a general relationship between the magnetic-induction decay and the viscosity field kinetics for an arbitrary number of half-periods of the square-wave field. The agreement of our theory with the experimental results turns out to be quite satisfactory. As consequence, the ordering processes responsible for the magnetic aftereffect in amorphous ferromagnets may be described as essentially uncorrelated.

I. INTRODUCTION

Preliminary results of measurements similar to the ones described in part I have been analyzed recently by introducing a specific theoretical model, where the ordering processes are considered as independent.¹ The hypothesis of existence of correlations between atomic ordering events was also considered.^{1,2}

By exploiting the complete set of measurements presently available, it is possible to critically consider the approach followed in the aforementioned papers. As a matter of fact, such a treatment may be applied only to aftereffect measurements performed at constant magnetic induction B , when the permeability variation with time originates from an increase in the value of the so-called viscosity field.³ Our measurements are, however, performed at constant driving-field amplitude. In these conditions, the magnetic induction B is observed to steadily decrease with time. The proposed approach retains validity only if the relative change in B during the measurement is sufficiently small [$\Delta B \ll B(\infty)$]. However, the observed variation of B between the time limits (t_1, t_2) of our aftereffect measurements is rather strong (see part I). It is therefore necessary to correctly compare the theoretical predictions with experimental results obtained under different dynamical conditions.

In Sec. II, the model's predictions for the viscosity-field variation at constant magnetic induction will be analyzed. Such a model allows one to evaluate the changes in the viscosity-field kinetics as a function of the number $2N$ of domain-wall cycles between positions (a) and (b) (see part I).

In Sec. III, the predictions of the proposed model will be exploited to justify the experimental results obtained in part I under different dynamical conditions for the domain walls. The proposed model will be shown to satisfactorily explain the complete set of experimental results, as a function of the number $2N$ of periodic domain-wall displacements, and of

the permanence time t^* of the walls in position (b) (see part I for details). The possible reasons for the slight discrepancy between experimental data and theoretical predictions will be examined in Sec. IV.

II. THEORY: VISCOSITY-FIELD CHANGE AT CONSTANT MAGNETIC INDUCTION

According to Néel, the viscosity field $H_{T,0}(B, t)$, acting on an oscillating domain wall, is a known function of the time t after domain nucleation and of the magnetic induction B , proportional to the amplitude of the domain-wall displacement.³ The dependence of $H_{T,0}$ on time and magnetic induction may be factorized as $H_{T,0}(B, t) = H_T(B)G_0(t)$, $G_0(t)$ being an increasing function of time, characterized by known initial and final values, $G_0(0) = 0$ and $G_0(\infty) = 1$.

Within the conventional model of independent ordering processes, each characterized by a time constant τ , this function may be written as

$$G_0(t) = 1 - \int_0^\infty p(\tau) \exp(-t/\tau) d\tau, \quad (1)$$

where $p(\tau)$ is a suitable distribution function. When a set of periodic ordering processes is considered, as explained in part I, the kinetics of the viscosity field is modified, and may be described by a different function, $G_{2N}(t)$, where N is the number of (a)-(b) cycles performed by the domain walls.

It is convenient to introduce two different time parameters: the total time t_{tot} elapsed since the removal of the saturating field, and an "inner" time t ($0 < t < t_0$) measured starting from every domain-wall displacement to position (a).

We assume that any ordering process related to the periodic presence or absence of a domain wall is characterized by a specific time constant τ (see Fig. 1). t_0 is the half-period of the square-wave field.

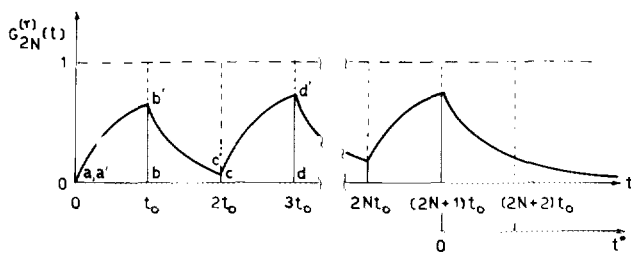


FIG. 1. Schematic behavior of $G_{2N}^{(r)}(t)$ as a function of the number of square-wave half-periods $2N$ and of waiting time t^* .

It may be easily verified that when the domain wall is in position (a), the time behavior of the viscosity field produced by the subset of ordering process characterized by the time constants τ is given by

$$G_{2N}^{(r)}(t) = 1 - F_{2N}(\tau) \exp(-t/\tau), \quad (2)$$

where

$$F_{2N}(\tau) = 1 - [\exp(t_0/\tau) - 1] \sum_{n=1}^N \exp[-2nt_0(1/\tau)] \\ = 1 - \frac{1 - \exp(-2Nt_0/\tau)}{1 + \exp(-t_0/\tau)} \exp(-t_0/\tau). \quad (3)$$

The function $F_{2N}(\tau)$ is a measure of the fraction of off-equilibrium defects which can still order at the time $2Nt_0$, i.e., once the domain wall has come back to position (a) after $2N$ half-periods of the square-wave field (see Fig. 1). The behavior of the viscosity field for a generic value of $2N$ is then

$$G_{2N}(t) = 1 - \int_0^\infty p(\tau) F_{2N}(\tau) \exp(-t/\tau) d\tau, \quad (4)$$

which is a straightforward generalization of Eq. (1).

We note explicitly that the value $G_{2N}(0)$ is zero only in the case $2N=0$, while for $2N \neq 0$, $G_{2N}(0) = 1 - \int_0^\infty p(\tau) F_{2N}(\tau) d\tau > 0$. Let us now examine the behavior of the viscosity field when the domain-wall cycling is interrupted [after $(2N+1)$ jumps] for a time t^* , during which the wall is left in position (b). After this time, the domain wall is brought back to position (a) by restoring the square-wave field. Our task is to find the intensity of the viscosity field at the time $t_{\text{tot}} = (2N+1)t_0 + t^*$ (see Fig. 1). Let us introduce the function $F_{2N}^{(R)}(\tau, t^*)$ measuring, by analogy with $F_{2N}(\tau)$, the total fraction of defects which can still order with time constant τ at the time $t_{\text{tot}} = (2N+1)t_0 + t^*$. It may be easily verified that

$$F_{2N}^{(R)}(\tau, t^*) = 1 - \frac{\{1 - \exp[-2(N+1)t_0/\tau]\}}{[1 + \exp(-t_0/\tau)]} \\ \times \exp(-t^*/\tau). \quad (5)$$

A precise relationship exists between the functions $F_{2N}(\tau)$ and $F_{2N}^{(R)}(\tau, t^*)$; in fact, $F_{2N+2}(\tau) = F_{2N}^{(R)}(\tau, t^* = t_0)$.

The time evolution of the viscosity field is now given by

$$G_{2N}^{(R)}(t) = 1 - \int_0^\infty p(\tau) F_{2N}^{(R)}(\tau, t^*) \exp(-t/\tau) d\tau, \quad (6)$$

where t is the time measured after the displacement of the wall back to position (a). The behavior of the functions

$F_{2N}(\tau)$ and $F_{2N=600}^{(R)}(\tau, t^*)$ is reported in Fig. 2. Four different values of τ are considered: $\tau = 0.5, 10, 10^2$, and 10^3 s.

III. MAGNETIC-INDUCTION CHANGE AT CONSTANT APPLIED FIELD

The expression for $G_{2N}(t)$ and $G_{2N}^{(R)}(t)$ derived in Sec. II must be properly handled in order to make a comparison of this theory with the experimental results of part I, obtained at constant magnetic field. As a matter of fact, the time behavior of the magnetic induction B during a typical aftereffect measurement is described by the simple equation

$$B(t) = \mu H_e - \mu H_T [B(t)] G(t), \quad (7)$$

where $\mu H_e = B_0(0)$, H_e is the external field, H_T is the viscosity field, and μ is the initial magnetic permeability.⁴

Equation (7) may be generalized in a straightforward manner to the case of a set of sequential decays,

$$B_{2N}(t) = \mu H_e - \mu H_T [B_{2N}(t)] G_{2N}(t), \quad (8)$$

where $\mu H_e = B_0(0)$. Note that this is an implicit equation for $B_{2N}(t)$, whose numerical solution requires the knowledge of the analytic behavior of the viscosity field as a function of $x = B_0(0)$. The function $G_{2N}(t)$ has been defined in Sec. II. The $H_T(x)$ curve has been derived elsewhere.⁵ It has been recently remarked⁴ that H_T may be closely approximated, in the whole interval of interest, by a simple analytic expression:

$$H_T(x) \simeq \alpha \sin[\pi x / (2B_m)], \quad x \lesssim \frac{1}{2} B_m, \quad (9)$$

where B_m corresponds to a domain-wall displacement of about one-quarter of the domain-wall thickness.⁵ The parameter $\alpha \approx N_D \epsilon_D^2 / (2I_s k_B T)$ contains information about the number N_D and coupling energy ϵ_D of defects; I_s is the alloy's saturation magnetization, and T is the absolute temperature.⁵

In order to determine the actual behavior of the function $G_{2N}(t)$ for the considered alloy, the time-constant distribution function $p(\tau)$ is to be evaluated from the time behavior of the relaxing magnetic induction, as discussed in a previous paper.⁴ In that case, the results were cast in the form of an activation-energy spectrum (or distribution of available processes) $q(E)$ by following the standard Primak's procedure.⁶ The relevant function is now $p(\tau)$, simply related to

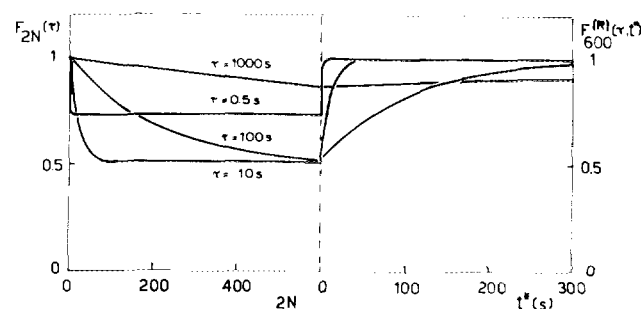


FIG. 2. Behavior of $F_{2N}(\tau)$ as a function of $2N$ and behavior of $F_{2N=600}^{(R)}(\tau, t^*)$ as a function of t^* for four different values of τ .

$q(E)$ by the relation $p(\tau)d\tau = q(E)dE$. Within this approach, τ is related to E by an Arrhenius equation of the type $\tau = \nu_0^{-1} \exp(E/k_B T)$, where ν_0 is an attack frequency. It should be noted that the functions $q(E)$ and $p(\tau)$ obtained by analyzing different samples of the same alloy are closely similar, although they may strongly differ in different alloys,⁴ allowing us to exploit the data for $q(E)$ obtained on the same amorphous ribbon and reported in Ref. 4. The function $p(\tau)$ corresponding at room temperature to the activation-energy spectrum determined for the $\text{Fe}_{81}\text{B}_{13.5}\text{Si}_{3.5}\text{C}_2$ alloy is shown in Fig. 3.

The behavior of the function $G_0(t)$ for this material is also well known.⁴ The functions $G_{2N}(t)$, $G_{2N}^{(R)}(t)$ for arbitrary values of $2N$ and/or t^* have been computed by inserting the $p(\tau)$ function into Eqs. (4) and (6) and by using the expressions for $F_{2N}(\tau)$ and $F_{2N}^{(R)}(\tau, t^*)$ given in Sec. II [Eqs. (3) and (5)]. The integration has been performed numerically. $G_{2N}(t)$ and $G_{2N}^{(R)}(t)$ have been used to evaluate $B_{2N}(t_1)$ and $B_{2N}(t_2)$ through Eq. (8). The values of $B_0(0)$, B_m , and the product $\mu\alpha$ have been determined on the basis of the results of extended-time measurements of the relaxation of B_0 .⁷ In fact, it has been experimentally verified that for a given material the relaxing quantity

$$D(t) = [B_0(t) - B_0(\infty)]/[B_0(0) - B_0(\infty)] \quad (10)$$

is essentially independent of the considered sample (while the various B_0 values measured under the same external field may vary from sample to sample, owing to differences in the magnetic domain structures). The complete $D(t)$ curve is known for the $\text{Fe}_{81}\text{B}_{13.5}\text{Si}_{3.5}\text{C}_2$ alloy, and is reported elsewhere.⁴ In particular, $D(t_1) = 0.926$ and $D(t_2) = 0.681$. As a consequence, it is possible to estimate the values of $B_0(0)$ and $B_0(\infty)$ for the sample used for the measurements of part I by inserting into Eq. (10) the average values of $B_0(t_2)$ and $B_0(t_1) = \Delta B_0 + B_0(t_2)$, and by using the known values of $D(t_1)$ and $D(t_2)$. As it turns out, $B_0(0) = 1.59 \times 10^{-4}$ T and $B_0(\infty) = 2.44 \times 10^{-5}$ T. The values of B_m and $\mu\alpha$ may now be obtained by using the simple procedure outlined in Ref. 4. In this case, the results are $B_m = 9.45 \times 10^{-5}$ T and $\mu\alpha = 3.43 \times 10^{-4}$ T.

These parameter values have been inserted into Eq. (8). The theoretical predictions for $B_{2N}(t_1)$ and $B_{2N}(t_2)$ as functions of both $2N$ and t^* (for $2N = 600$) are shown in

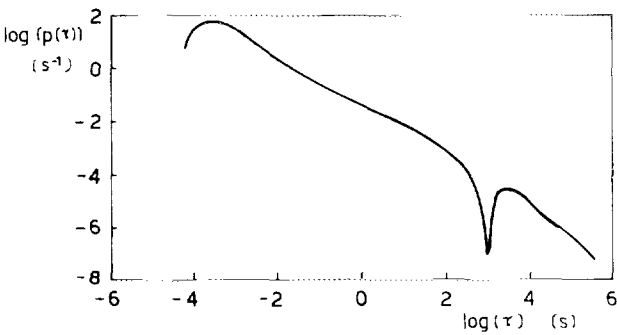


FIG. 3. Behavior of the time-constant distribution function $p(\tau)$ for amorphous $\text{Fe}_{81}\text{B}_{13.5}\text{Si}_{3.5}\text{C}_2$ at room temperature.

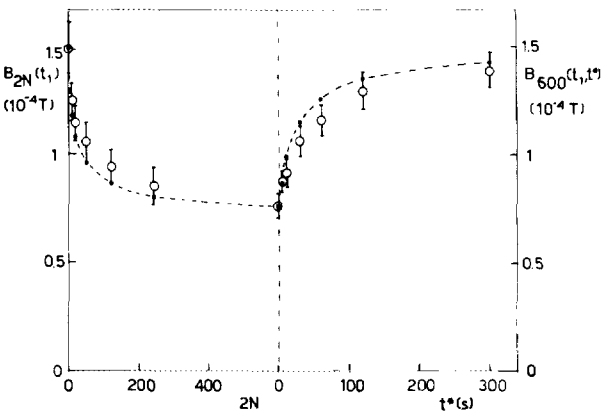


FIG. 4. Direct and reverse relaxation of $B_{2N}(t_1)$. Dashed lines: theoretical results (note that strictly speaking the curve for the direct relaxation is not a continuous one); the full symbols evidence the theoretical results corresponding to the actual measurements. Open circles: experimental data.

Figs. 4 and 5 (full symbols). It should be noted that the values of $B_{2N}(t_i)$ approach a lower limiting value for $2N \rightarrow \infty$. In fact, $F_{2N}(\tau)$ reduces to $1/[1 + \exp(-t_0/\tau)]$ in this limit [see Eq. (3)]. It turns out that $B_{2N \rightarrow \infty}(t_1) = 4.94 \times 10^{-5}$ T and $B_{2N \rightarrow \infty}(t_2) = 4.58 \times 10^{-5}$ T.

It should be remarked that the theoretical curves of Figs. 4 and 5 have been obtained by introducing a minimum amount of physical or mathematical approximations [such as the ones involved in the standard Primak's procedure,⁶ and the use of Eq. (9) for $H_T(x)$]. Moreover, no free parameters are involved, all parameter values being unequivocally determined. Small errors may come from numerical treatment of the data, particularly the integration of Eqs. (4) or (6).

IV. DISCUSSION

The experimental data for $B_{2N}(t_2)$ and $B_{2N}(t_1) = B_{2N}(t_2) + \Delta B_{2N}$, taken from Figs. 6 and 7 of part I, have been plotted in Figs. 4 and 5 for direct and reverse relaxation processes (open circles). The error bars are also shown. The agreement between these results and the

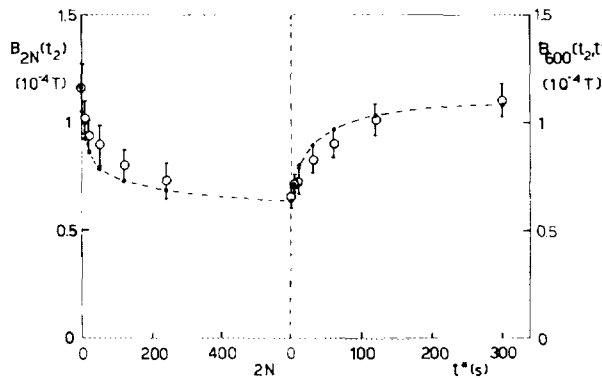


FIG. 5. Same as in Fig. 4 for $B_{2N}(t_2)$.

predictions of our model is fairly good. We conclude therefore that the considered model of independent ordering processes appears to correctly explain the time evolution of the magnetic-induction aftereffect as a function of the number of half cycles of the square-wave field. Furthermore, the reverse relaxation of B towards the initial value, observed by interrupting the domain-wall cycling for a time t^* , is qualitatively understood in terms of the same model.

However, the agreement between theoretical values and experimental data is satisfactory but not absolute. For many values of $2N$ or t^* , in fact, the theoretical predictions fall slightly off the standard-deviation bars of the corresponding measurements. The theoretical curves for both direct and reverse relaxation of $B_{2N}(t_1)$ and $B_{2N}(t_2)$ appear to systematically follow a faster kinetics than the measured data. Such a slight but definite discrepancy could be ascribed to the inadequacy of the simple model of independent ordering events. However, a less fundamental explanation is also possible: in fact, the $p(\tau)$ function shown in Fig. 3 was obtained by using the standard Primak's procedure, involving, as is well known,⁸ analytical and numerical approximations which affect to some extent the final result. It cannot therefore be excluded that the experimental data could be more closely reproduced through a better evaluation of the time-constant distribution function, $p(\tau)$.

Let us finally remark that in some previous works^{1,2} the progressive reduction in the slope of the magnetic-induction aftereffect ΔB_{2N} observed with increasing $2N$ (see Fig. 6 of part I) was assumed as a proof of the inadequacy of the model of independent ordering processes in the case of amorphous ferromagnets. The results of the present analysis indicate instead that when the effect of the progressive changes of H_T [Eq. (4)] on the magnetic induction B is properly

taken into account, the reduction of $B_{2N}(t_1)$ and $B_{2N}(t_2)$ with increasing $2N$ is correctly explained by the considered model, which therefore accounts also for the observed reduction in the slope of $\Delta B_{2N} = B_{2N}(t_1) - B_{2N}(t_2)$.

A central point of the present investigation has been the recognition that the model discussed in Sec. II can be directly checked only on permeability-relaxation results obtained at constant B . In conventional measurements performed at constant applied field H_e , the model may still be used without substantial modifications only for materials exhibiting an aftereffect $\Delta B \ll B(\infty)$. This is, however, not the case for most amorphous ferromagnetic alloys, as experimentally verified.⁷ For these materials, the procedure proposed in Ref. 4 and used in the present work is required. The theoretical curves may, however, be affected by some uncertainty, deriving from the numerical and analytical approximations involved in the calculations. Measurements at constant B , like the ones performed by Wang and Ho in a different experiment,⁹ would undoubtedly provide the most direct and accurate way to check a particular model for the microscopic mechanisms of directional ordering in ferromagnetic amorphous alloys.

¹ P. Allia, C. Beatrice, P. Mazzetti, and F. Vinai, *J. Appl. Phys.* **63**, 829 (1988).

² P. Allia, C. Beatrice, and F. Vinai, in *Fundamental and Applicative Aspects of Disordered Magnetism*, edited by P. Allia, D. Fiorani, and L. Lanotte (World Scientific, Singapore, 1989), p. 104.

³ L. Néel, *J. Phys. Rad.* **15**, 225 (1954).

⁴ P. Allia, *J. Magn. Magn. Mater.* **82**, 77 (1989).

⁵ P. Allia and F. Vinai, *IEEE Trans. Magn.* **MAG-17**, 1481 (1981).

⁶ W. Primak, *Phys. Rev.* **100**, 1677 (1955).

⁷ P. Allia, C. Beatrice, and F. Vinai, *Philos. Mag.* (in press).

⁸ M. R. J. Gibbs, J. E. Evetts, and J. A. Leake, *J. Mater. Sci.* **18**, 278 (1983).

⁹ Q. Wang and K.-Y. Ho, *Mater. Sci. Eng.* **97**, 529 (1988).